

Virtual Knot Diagrams and the  
Witten-Reshetikhin-Turaev Invariant

H. A. Dye

MADN-MATH

United States Military Academy

646 Swift Road

West Point, NY 10996

hdye@ttocs.org

Louis H. Kauman

Department of Mathematics, Statistics, and Computer Science

University of Illinois at Chicago

851 South Morgan St

Chicago, IL 60607-7045

kau man@uic.edu

Abstract

The Witten-Reshetikhin-Turaev invariant of classical link diagrams is generalized to virtual link diagrams. This invariant is unchanged by the framed Reidemeister moves and the Kirby calculus. As a result, it is also an invariant of the 3-manifolds represented by the classical link diagrams. This generalization is used to demonstrate that there are virtual knot diagrams with a non-trivial Witten-Reshetikhin-Turaev invariant and trivial 3-manifold fundamental group.

## 1 Introduction

Generalizations of the Jones polynomial have been defined for virtual link diagrams [9], [3], [12]. We continue this process by generalizing the Witten-Reshetikhin-Turaev invariant and the colored Jones polynomials to virtual link diagrams. The Witten-Reshetikhin-Turaev invariant of classical link diagrams is unchanged by the framed Reidemeister moves. It is also 3-manifold invariant and is unchanged by the Kirby calculus. This invariant is a weighted sum of colored Jones polynomials. Our generalization will also be a weighted sum of colored Jones polynomials and invariant under the framed Reidemeister moves and a generalization of the Kirby calculus.

Every framed, classical link diagram represents a 3-manifold via framed surgery performed on that link. Two 3-manifolds represented by link diagrams

are homeomorphic if and only if their diagrams are related by a sequence of framed Reidemeister moves and Kirby calculus moves. The fundamental group of this 3-manifold can be computed from a corresponding link diagram. As a result, we can formally extend the definition of the 3-manifold group to a virtual link diagram. We define a virtual Kirby calculus by generalizing the moves of Kirby calculus to incorporate virtual crossings.

The 3-manifold group of a virtual link diagram is invariant under the framed Reidemeister moves, the virtual Reidemeister moves, and the virtual Kirby calculus. This invariance gives rise to the concept of 'virtual 3-manifolds'. Virtual link diagrams appear to have the same structure as classical link diagrams (that specify 3-manifolds), but virtual 3-manifolds (specified by non-classical virtual diagrams) have no corresponding surgery construction. A virtual 3-manifold is, by definition, an equivalence class of link diagrams related by the framed Reidemeister moves, virtual Reidemeister moves, and virtual Kirby calculus.

In this paper, we recall virtual knot theory in section 2. We recall the definitions of the virtual fundamental group and the generalized Jones polynomial. Then, we define the 3-manifold group of a virtual link diagram using the definition of the virtual fundamental group. We prove that the 3-manifold group of a virtual link diagram is invariant under the framed Reidemeister moves, virtual Reidemeister moves and the Kirby calculus.

In section 3, we recall the definition of the colored Jones polynomial of a virtual link diagram. We use this definition to define the Witten-Reshetikhin-Turaev invariant of a virtual link diagram. We introduce several formulas that reduce the computational complexity of the Witten-Reshetikhin-Turaev invariant. Finally, we prove that the Witten-Reshetikhin-Turaev invariant is invariant under the Kirby calculus.

The reader should note that all formulas in the paper that are written in the form of a graphical equation are formulas that indicate the possibility of a substitution of one type of graphic for another graphic in a link diagram. The equality in the equation means that the bracket evaluation of the two diagrams are equal.

We compute the Witten-Reshetikhin-Turaev invariant of two virtual knot diagrams in the next section. The fundamental group of these virtual knot diagrams is  $\mathbb{Z}$ . The 3-manifold group of one of the virtual knot diagrams is the trivial group. However, the Witten-Reshetikhin-Turaev invariant of this virtual knot diagram is non-trivial. This produces a virtual counterexample to the Poincaré conjecture.

In the final section, we discuss the difficulties of computing the Witten-Reshetikhin-Turaev invariant in the virtual case. We observe that in order to compute the Witten-Reshetikhin-Turaev invariant of a virtual link diagram, we must compute the Jones polynomial of some complicated virtual link diagrams. The formulas given in sections 3 and 4 were computed using Temperley-Lieb recoupling theory. The full machinery of recoupling theory does not generalize to the virtual case. We present several propositions that highlight the difficulty of computing formulas that include virtual crossings.

## 2 Virtual Knot Diagrams

Virtual knot theory is a generalization of classical knot theory introduced by Louis H. Kauffman in 1996 [9]. In this section, we review classical and virtual knot theory. We then recall several classical knot invariants that have been generalized to virtual knot diagrams.

A classical knot diagram is a decorated immersion of  $S^1$  into the plane with over/under markings at each crossing. Two classical knot diagrams are said to be equivalent if one may be transformed into another by a sequence of Reidemeister moves. Local versions of the Reidemeister move are illustrated in Figure 1.

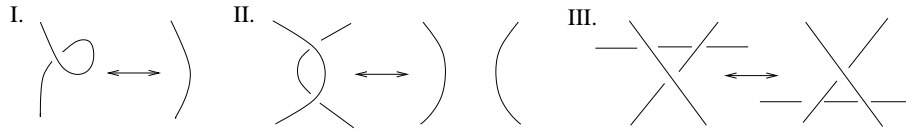


Figure 1: Reidemeister moves

A virtual knot diagram is a decorated immersion of  $S^1$  into the plane with two types of crossings: classical and virtual. Classical crossings are indicated by over/under markings and virtual crossings are indicated by a solid encircled X. Two virtual knot diagrams are said to be equivalent if one may be transformed into the other via a sequence of Reidemeister moves and virtual Reidemeister moves. The virtual Reidemeister moves are illustrated in Figure 2. Note that the classical knot diagrams are a subset of the virtual knot diagrams.

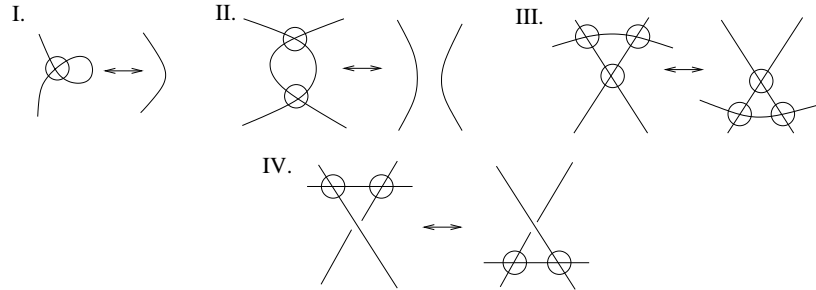


Figure 2: Virtual Reidemeister moves

The virtual Reidemeister moves can be constructed from a single diagrammatic move: the detour move. The detour move pertains only to virtual crossings and is performed in the following way. Choose an orientation of the virtual knot diagram for convenience. Select two points,  $a$  and  $b$ , on the virtual knot diagram. The arc from  $a$  to  $b$ , in the direction of the orientation, contains only virtual crossings and no classical crossings. Otherwise we may not perform the detour move. (This condition is illustrated in Figure 3.) Remove the arc of the

knot diagram from point  $a$  to point  $b$ , and insert any new arc that does not create triple points. All double points produced by the placement of the new arc are virtual crossings.

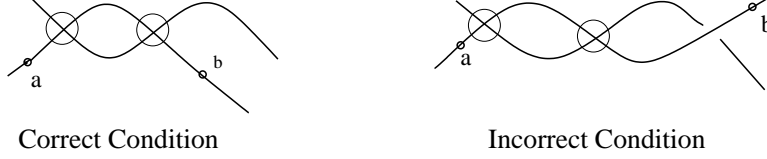


Figure 3: The detour move condition

**Proposition 2.1.** The detour move is equivalent to a sequence of virtual Reidemeister moves.

**Remark 2.1.** We sketch the proof of this proposition. A large scale move like the detour move may be broken down in a series of smaller sequential moves. These smaller moves involve at most three crossings. Note that each virtual Reidemeister move is a detour move.

**Remark 2.2.** Equivalence classes of virtual knot diagrams are in one to one correspondence with equivalence classes of embeddings of  $S^1$  into thickened, oriented 2-dimensional surfaces [6], [11] and [2]. A surface with an embedded  $S^1$  is equivalent to a (possibly different) surface with an embedded  $S^1$  if one surface with an embedding can be transformed into the other by a sequence of homeomorphisms of the surface, handle cancellations and additions (to the surface), and Reidemeister moves in the surface.

A virtual  $n$ -tangle diagram is a decorated immersion of  $n$  copies of  $[0;1]$  with classical and virtual crossings. The  $2n$  endpoints of the diagram are arranged so that  $n$  endpoints appear in a row at the top and  $n$  endpoints form a lower row. Note that it is possible to construct tangle diagrams with no crossings. The closure of an  $n$ -tangle,  $T$  connects each upper endpoint with a corresponding lower endpoint as illustrated in figure 4.

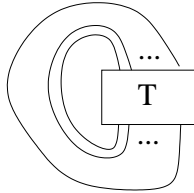


Figure 4: The closure of an  $n$ -tangle

We now recall the definition of several invariants of virtual knot diagrams. These invariants will be referred to throughout this paper. The writhe of a

virtual knot diagram and the linking number of a virtual link diagram are computed from an oriented diagram. To define these invariants, we introduce the sign (crossing sign) of a classical crossing. Each classical crossing in a virtual



Figure 5: Crossing sign

knot diagram can be assigned a crossing sign. To compute the crossing sign, we orient the knot diagram. Each classical crossing is assigned a value based on the orientation as shown in Figure 5. Let  $v$  be a classical crossing in a virtual knot diagram. We denote the crossing sign of  $v$  as  $\text{sgn}(v)$ . The writhe of a virtual knot diagram  $K$  is determined by the crossing sign of each classical crossing in the diagram. We denote the writhe of  $K$  as  $w(K)$ .

$$w(K) = \sum_{v \in K} \text{sgn}(v)$$

The Reidemeister I move changes the writhe of a knot diagram. An unknot with a single Reidemeister I move, is referred to as a 1 framed unknots based on the sign of the crossing. (We illustrate 1 framed unknots in Figure 6.) The Reidemeister II and III moves do not change the writhe of a knot diagram and are referred to as the framed Reidemeister moves. Two classical knot diagrams that are related by a sequence of Reidemeister II and III moves are said to be regularly isotopic.

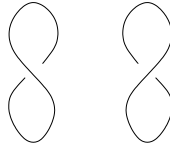


Figure 6: 1 Framed unknots

The linking number of an oriented two component virtual link diagram with oriented components,  $L_1$  and  $L_2$ , is denoted  $\text{lk}(L_1; L_2)$ . Let  $U$  denote the set of all classical crossings formed by the components  $L_1$  and  $L_2$ . Then the linking number is defined by the formula:

$$\text{lk}(L_1; L_2) = \sum_{v \in U} \frac{\text{sgn}(v)}{2} : \quad (1)$$

Note that  $\text{lk}(L_1; L_2) = \text{lk}(L_2; L_1)$ .

Remark 2.3. There is an alternative definition of writhe where  $lk(L_1; L_2)$  and  $lk(L_2; L_1)$  are not necessarily equivalent [4].

We recall the fundamental group and the longitude of a virtual knot diagram. These definitions are used to generalize the 3-manifold group obtained from a classical knot diagram to virtual knot diagrams.

The fundamental group of a virtual knot diagram is a free group modulo relations determined by the classical crossings in the diagram. Each segment of the diagram starts and terminates at classical crossings (possibly passing through virtual crossings). We assign each segment a label. These labels represent the generators of the free group. From each crossing we obtain a relation as illustrated in Figure 7.

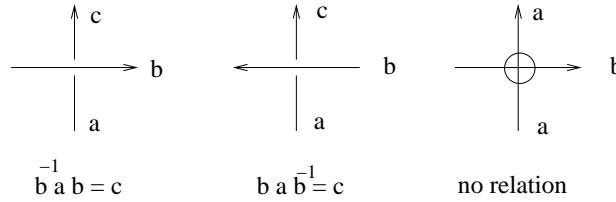


Figure 7: Relations determined by crossings

The fundamental group of a virtual knot diagram is invariant under the Reidemeister moves and virtual Reidemeister moves.

A longitude of a virtual knot diagram is a word of the form  $l_1^{-1} l_2^{-1} \dots l_1^{-1}$  where each  $l_i$  is one of the generators of the fundamental group. We compute a longitude by choosing an initial point on the diagram. We traverse the virtual knot diagram from the initial point in the direction of its orientation. We record either  $b$  or  $b^{-1}$  as we traverse an underpass under the arc  $b$ . We determine whether to record  $b$  or  $b^{-1}$  as shown in Figure 8. The longitude of a virtual knot diagram is determined up to cyclic permutation of its members.

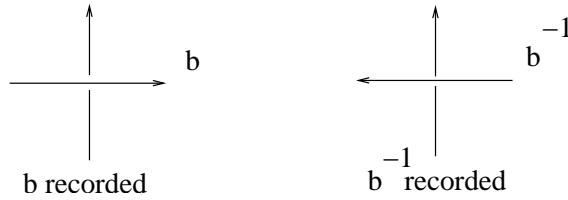


Figure 8: Longitude determined by crossings

The three-manifold group of a virtual knot diagram  $K$ ,  $\pi_3(K)$ , is the fundamental group modulo the longitude. The three-manifold group is invariant under the Reidemeister moves II and III, the virtual Reidemeister moves, and the Kirby calculus. The virtual Kirby calculus consists of two moves: the introduction and deletion of 1 framed unknots and handle sliding. We describe a

handle slide for a framed virtual link diagram  $K$  with at least two components,  $A$  and  $B$ . Diagrammatically, handle slide  $A$  over  $B$  by the following process. Replace  $B$  with two parallel copies of  $B$ . Take the connected sum of  $A$  and the outermost copy of  $B$ .

We show an example of this process in Figure 9, where a  $+1$  framed unknot is slid over a trefoil.

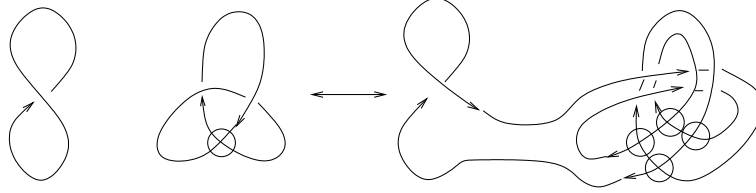


Figure 9: A example of a handle slide with virtual crossings

These two moves are called the Kirby moves.

Remark 2.4. In the case of classical link diagrams, the definition of the classical Kirby calculus is identical to the definition given above without virtual crossings.

Remark 2.5. The following question has been posed: if two classical diagrams are equivalent under the virtual Kirby calculus, are they equivalent under the classical Kirby calculus.

The 3-manifold group is invariant under the framed Reidemeister moves and the virtual Reidemeister moves. It remains to prove that the 3-manifold group is invariant under the Kirby moves.

A classical framed link diagram represents the three manifold obtained by removing a small neighborhood of each component of the link diagram, and gluing in a solid torus so that the meridian is identified with the longitude of the removed link component [13]. The Reidemeister I move changes the longitude of a knot diagram and changes the identification used to glue in the torus.

For example, the fundamental group of an unknot with writhe 0 and the fundamental group of a  $-1$  framed unknot are both  $\mathbb{Z}$ . However, the 3-manifold group of an unknot with writhe zero is  $\mathbb{Z}$  and the three-manifold group of the  $-1$  framed unknot is the trivial group. The unknot with writhe 0 represents  $S^1 \times S^2$  and the  $-1$  framed unknot represents  $S^3$ .

Theorem 2.2. If two classical framed link diagrams,  $K$  and  $\hat{K}$ , are related by a sequence of Kirby moves and framed Reidemeister moves then

$$\pi_1(M(K)) = \pi_1(M(\hat{K}))$$

and the two diagrams represent homeomorphic three manifolds.

Proof: [13]. ■

Theorem 2.3. The 3-manifold group of a virtual knot diagram  $K$ , is invariant under the framed Reidemeister moves, the virtual Reidemeister moves (detour move) and the Kirby calculus.

Proof: The fundamental group is not changed by the framed Reidemeister moves and the virtual Reidemeister moves. The longitude is also unchanged by the Reidemeister II and III moves and the detour move. This implies that the 3-manifold group of a virtual knot diagram is not changed by these moves. We only need to show that the 3-manifold group is unchanged by the Kirby moves.

The 3-manifold group of a 1 framed unknot is trivial and the introduction of a disjoint 1 framed unknot to the diagram does not change the 3-manifold group.

We consider the effect of handle sliding on a virtual knot diagram. Consider a virtual knot diagram with two disjoint components, oriented as shown in figure 10. Denote the two components by  $K_1$  and  $K_2$ , the 3-manifold group by  ${}_M(K_1 \sqcup K_2)$ , and the longitudes of  $K_1$  and  $K_2$  as  $L_1$  and  $L_2$ . Assume that the arcs of  $K_1$  are labeled sequentially as  $Z; Z_1; Z_2 :: Z_m$  in the direction of orientation. The placement of the labeled arc  $Z$  is indicated in figure 10. Similarly, the arcs of the component  $K_2$  are labeled in the direction of orientation as  $A_1; A_2; :: A_n$ . (To generalize the argument, we would consider the different possible orientations of  $K_1$  and  $K_2$ , and the case where  $K_2$  is a link with multiple components.)

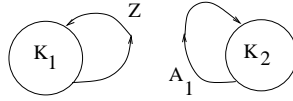


Figure 10: Two virtual knot diagrams before a handle slide

Handle slide  $K_1$  over  $K_2$ , and we obtain the diagram shown in figure 11. Let  $\hat{K}$  denote the new diagram,  ${}_M(\hat{K})$  the corresponding 3-manifold group, and  $\hat{L}_1$  and  $\hat{L}_2$  the new longitudes.

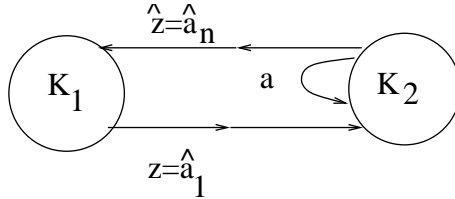


Figure 11: Two virtual knot diagrams after a handle slide

The virtual crossings do not produce any new relations, therefore we need only examine the effect of the handle slide on the classical crossings. Each original crossing in  $K_1$  is unchanged. Each classical crossing in  $K_2$  becomes a set of four classical crossings whose four relations reduce to a single equation. Consider a positive crossing in  $K_2$  as shown in figure 12.



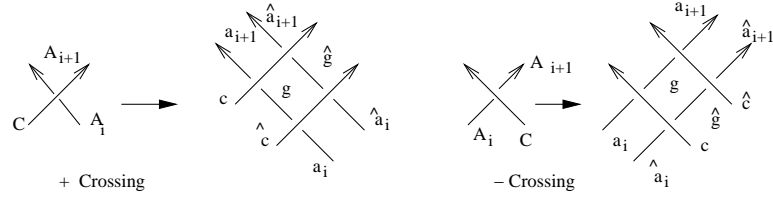


Figure 12: Detail of a crossing before and after a handle slide

We obtain the following relationship from a positive classical crossing before handle sliding:  $C^{-1}A_iC = A_{i+1}$ . After handle sliding, we obtain four relations from the positive crossing.

$$\begin{aligned} c^{-1}gc &= a_{i+1} & c^{-1}\hat{g}c &= \hat{a}_{i+1} \\ \hat{c}^{-1}a_i\hat{c} &= g & \hat{c}^{-1}\hat{a}_i\hat{c} &= \hat{g} \end{aligned}$$

These equations may be simplified to two equations:

$$\begin{aligned} c^{-1}\hat{c}^{-1}a_i\hat{c} &= a_{i+1} \\ c^{-1}\hat{c}^{-1}\hat{a}_i\hat{c} &= \hat{a}_{i+1} \end{aligned}$$

Multiplying, we obtain a single relation from each set of four positive crossings:

$$(\hat{c}c)^{-1}(\hat{a}_ia_i)(\hat{c}c) = \hat{a}_{i+1}a_{i+1}$$

The change for negative classical crossing is also shown in Figure 12. We also obtain a single relation in the case of a negative crossing.

$$(\hat{c}c)(\hat{a}_ia_i)(\hat{c}c)^{-1} = \hat{a}_{i+1}a_{i+1}$$

Consider the longitude of  $K_2$ . Compute the original longitude by traversing the knot starting at  $A_1$ . If  $L_2 = f x_1^{-1}; x_2^{-1} :: x_n^{-1} g$  then

$$\hat{L}_2 = f(x_1^{-1}x_1)^{-1}; (x_2^{-1}x_2)^{-1} :: (x_n^{-1}x_n)^{-1} g;$$

Hence,  $\hat{L}_2 a_1 z \hat{L}_2^{-1} = a_1 z$  implies that  $z = \hat{z}$ . Further, if  $L_1$  is computed by traversing the knot from  $z$  in the direction of the orientation, then we observe that  $\hat{L}_1 = L_1 \hat{L}_2$ . These computations allow us to conclude that  $\mu_M(K) = \mu_M(\hat{K})$ . ■

We recall a generalization of the bracket model [7] to define the generalized Jones polynomial of a virtual knot diagram. Each classical crossing may be smoothed as a type smoothing or a type smoothing as illustrated in Figure 13.

A state of a virtual knot diagram is a diagram determined by a choice of smoothing type for each classical crossing. Note that a state of a virtual link diagram may contain virtual crossings and consists of closed curves (possibly) with virtual crossings.

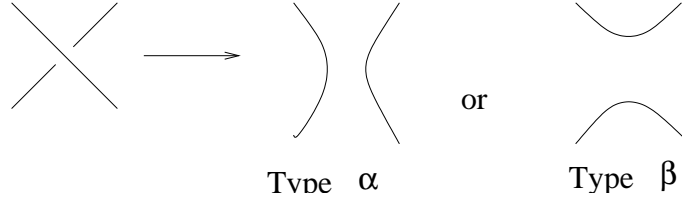


Figure 13: Smoothing types

Let  $K$  be a virtual knot diagram. Let  $s$  be a state of the virtual knot diagram, let  $S$  represent the set of all possible states and let  $c(s)$  equals the number of type  $\alpha$  crossings minus the number of type  $\beta$  crossings. Let  $|s|$  denote the number of closed curves in the smoothed diagram and  $d = (A^2 + A^{-2})$ . The bracket polynomial of  $K$  denoted  $\langle K \rangle$  is then:

$$\langle K \rangle = \sum_{s \in S} d^{|s|} A^{c(s)}$$

The bracket polynomial is invariant under the Reidemeister II and III moves and the virtual Reidemeister moves. To obtain invariance under the Reidemeister I move, we use the writhe of  $K$  to normalize. We define the normalized bracket polynomial of a virtual knot diagram.

$$f_K(A) = (-A)^{-3w(K)} \langle K \rangle$$

The only difference between this definition and the definition of the classical Jones polynomial is that a state of virtual knot diagram is set of closed curves (possibly containing virtual crossings) and not a set of simple closed curves. The Jones polynomial,  $V_K(t)$ , and the bracket polynomial are related by letting  $A = t^{1/4}$ .

$$f_K(t^{1/4}) = V_K(t) \quad (2)$$

In the next section, we introduce the Witten-Reshetikhin-Turaev invariant. This invariant will be generalized to virtual knot diagrams and is invariant under the Kirby calculus, framed Reidemeister moves, and the virtual Reidemeister moves.

### 3 The Witten-Reshetikhin-Turaev Invariant

In this section, we extend the definition of the Witten-Reshetikhin-Turaev invariant [16], [14], [15] to virtual link diagrams. First, we recall the definition of the Jones-Wenzl projector (q-symmetrizer) [10]. We then define the colored Jones polynomial of a virtual link diagram. It will be clear from this definition that two equivalent virtual knot diagrams have the same colored Jones polynomial. We will use these definitions to extend the Witten-Reshetikhin-Turaev invariant to virtual link diagrams. From this construction, we conclude that

two virtual link diagrams, related by a sequence of framed Reidemeister moves and virtual Reidemeister moves, have the same Witten-Reshetikhin-Turaev invariant. Finally, we will prove that the generalized Witten-Reshetikhin-Turaev invariant is unchanged by the virtual Kirby calculus. In the next section, we present two virtual knot diagrams that have fundamental group  $\mathbb{Z}$  and a Witten-Reshetikhin-Turaev invariant that is not equivalent to 1.

To form the  $n$ -cabling of a virtual knot diagram, take  $n$  parallel copies of the virtual knot diagram. A single classical crossing becomes a pattern of  $n^2$  classical crossings and a single virtual crossing becomes  $n^2$  virtual crossings.

Let  $r$  be a fixed integer such that  $r \geq 2$  and let

$$A = e^{\frac{i}{2r}} :$$

Here is a formula used in the construction of the Jones-Wenzl projector.

$$P_n = (-1)^n \frac{A^{2n+2} - A^{-(2n+2)}}{A^2 - A^{-2}} :$$

Note that  $P_1 = (A^2 + A^{-2})$ , the value assigned to a simple closed curve by the bracket polynomial. There will be an analogous interpretation of  $P_n$  which we will discuss later in this section.

We recall the definition of an  $n$ -tangle. Any two  $n$ -tangles can be multiplied by attaching the bottom  $n$  strands of one  $n$ -tangle to the upper  $n$  strands of another  $n$ -tangle. We define an  $n$ -tangle to be elementary if it contains no classical or virtual crossings. Note that the product of any two elementary tangles is elementary. Let  $I$  denote the identity  $n$ -tangle and let  $U_i$  such that  $i \in \{1, 2, \dots, n\}$  denote the  $n$ -tangles shown in Figure 14. By multiplying

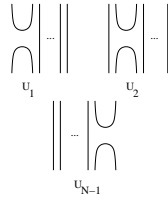


Figure 14: Elementary  $n$ -tangles

a finite set of  $U_{i_1} U_{i_2} \dots U_{i_n}$ , we can obtain any elementary  $n$ -tangle. Formal sums of the elementary tangles over  $\mathbb{Z}[A; A^{-1}]$  generate the  $n^{\text{th}}$  Temperley-Lieb algebra [10].

We recall that the  $n^{\text{th}}$  Jones-Wenzl projector is a certain sum of all elementary  $n$ -tangles with coefficients in  $\mathbb{C}$  [10], [8]. We denote the  $n^{\text{th}}$  Jones-Wenzl projector as  $T_n$ . We indicate the presence of the Jones-Wenzl projector and the  $n$ -cabling by labeling the component of the knot diagram with  $n$ .

**Remark 3.1.** There are different methods of indicating the presence of a Jones-Wenzl projector. In a virtual knot diagram, the presence of the  $n^{\text{th}}$  Jones-Wenzl

projector is indicated by a box with  $n$  strands entering and  $n$  strands leaving the box. For  $n$ -cabled components of a virtual link diagram with a attached Jones-Wenzl projector, we indicate the cabling by labeling the component with  $n$  and the presence of the projector with a box. This notation can be simplified to the convention indicated in the definition of the colored Jones polynomial. The choice of notation is dependent on the context.

We construct the Jones-Wenzl projector recursively. The 1<sup>st</sup> Jones-Wenzl projector consists of a single strand with coefficient 1. The is exactly one 1-tangle with no classical or virtual crossings. The  $n^{\text{th}}$  Jones-Wenzl projector is constructed from the  $(n-1)^{\text{th}}$  and  $(n-2)^{\text{th}}$  Jones-Wenzl projectors as illustrated in figure 15.

$$\boxed{q} = \boxed{q-1} - \frac{\Delta_{q-2}}{\Delta_{q-1}} \left( \text{diagram of two } \boxed{q-1} \text{ boxes connected by a crossing} \right)$$

Figure 15:  $n^{\text{th}}$  Jones-Wenzl projector

We use this recursion to construct the 2<sup>nd</sup> Jones-Wenzl projector as shown in figure 16.

$$\boxed{2} = \text{two parallel strands} - \frac{\Delta_0}{\Delta_1} \left( \text{diagram of two strands forming a cup and a cap} \right)$$

Figure 16: 2<sup>nd</sup> Jones-Wenzl projector

We will refer to the Jones-Wenzl projector as the J-W projector for the remainder of this paper.

We review the properties of the J-W projector. Recall that  $T_n$  denotes the  $n^{\text{th}}$  J-W projector then

- i)  $T_n T_m = T_n$  for  $n \leq m$
- ii)  $T_n U_i = 0$  for all  $i$
- iii) The bracket evaluation of the closure of  $T_n = \frac{1}{n}$

Remark 3.2. The combinatorial definition of the J-W projector is given in [10], p. 15. Note that [10] provides a full discussion of all formulas given above.

Let  $K$  be a virtual link diagram with components  $K_1; K_2 :: K_n$ . Fix an integer  $r \geq 2$  and let  $a_1; a_2 :: a_n \in \{0; 1; 2; :: r-2\}$ . Let  $\mathbf{a}$  represent the vector  $(a_1; a_2; :: a_n)$ . Fix  $A = e^{\frac{1}{2r}}$  and  $d = A^2 - A^{-2}$ . We denote the generalized a-colored Jones polynomial of  $K$  as  $hK^{\mathbf{a}}i$ . To compute  $hK^{\mathbf{a}}i$ , we cable the component  $K_i$  with  $a_i$  strands and attach the  $a_i^{\text{th}}$  J-W projector to cabled component  $K_i$ . We apply the Jones polynomial to the cabled diagram with attached J-W projectors.

The colored Jones polynomial is invariant under the framed Reidemeister moves and the virtual Reidemeister moves. This result is immediate, since the Jones polynomial is invariant under the framed Reidemeister moves and the virtual Reidemeister moves.

Remark 3.3. The a-colored Jones polynomial of the unknot is  $\frac{1}{A}$ . In other words, the Jones polynomial of the closure of the  $a^{\text{th}}$  J-W projector is  $\frac{1}{A}$ .

The generalized Witten-Reshetikhin-Turaev invariant of a virtual link diagram is a sum of colored Jones polynomials. Let  $K$  be a virtual knot diagram with  $n$  components. Fix an integer  $r \geq 2$ . We denote the unnormalized Witten-Reshetikhin-Turaev invariant of  $K$  as  $hK^{\mathbf{a}}i$ , which is shorthand for the following equation.

$$hK^{\mathbf{a}}i = \sum_{a_1, a_2, ::, a_n \in \{0; 1; 2; :: r-2\}} hK^{\mathbf{a}}i \quad (3)$$

Remark 3.4. For the remainder of this paper, the Witten-Reshetikhin-Turaev invariant will be referred to as the WRT.

We define the matrix  $N$  in order to construct the normalized WRT [10]. Let  $N$  be the matrix defined as follows:

$$i) N_{ij} = \text{lk}(K_i; K_j) \text{ for } i \neq j$$

$$ii) N_{ii} = w(K_i)$$

then let

$$b_+(K) = \text{the number of positive eigenvalues of } N$$

$$b_-(K) = \text{the number of negative eigenvalues of } N$$

$$n(K) = b_+(K) - b_-(K):$$

The normalized WRT of a virtual link diagram  $K$  is denoted as  $Z_K(r)$ . Let  $A = e^{\frac{1}{2r}}$  and let  $j, k$  denote the number of components in the virtual link diagram  $K$ . Then  $Z_K(r)$  is defined by the formula

$$Z_K(r) = hK^{\mathbf{a}}i \cdot A^{j+1-n(K)}$$

where

$$= \frac{r}{2} \sin\left(\frac{\pi}{r}\right)$$

and

$$= (-i)^r \cdot 2e^{i \left[ \frac{3(r-2)}{4r} \right]}.$$

This normalization is chosen so that normalized WRT of the unknot with writhe zero is 1 and the normalization is invariant under the introduction and deletion of  $\pm 1$  framed unknots.

Let  $\hat{U}$  be a  $a+1$  framed unknot. We recall that  $\hat{U} = h\hat{U}^{\pm 1}$  [10], page 146. Since  $\hat{U}$  and  $K$  are disjoint in  $K \# \hat{U}$  then  $h(K \# \hat{U})^{\pm 1} = hK^{\pm 1} h\hat{U}^{\pm 1}$ . We note that  $b_{\pm}(K \# \hat{U}) = b_{\pm}(K) + 1$ ,  $b_{\pm}(K \# \hat{U}) = b_{\pm}(K)$ , and  $\#(K \# \hat{U}) = \#K + 1$ . We compute that

$$Z_{K \# \hat{U}}(r) = hK^{\pm 1} h\hat{U}^{\pm 1} r^{\#K + 2 - n(K) - 1}$$

As a result,

$$Z_{K \# \hat{U}}(r) = Z_K(r):$$

We demonstrate that the normalized, generalized WRT is invariant under the framed Reidemeister moves and the Kirby calculus. The WRT is a sum of colored Jones polynomials and it is clear that the WRT is invariant under the framed Reidemeister moves and the virtual Reidemeister moves. In particular, the normalized WRT is invariant under the first Kirby move (the introduction and deletion of  $\pm 1$  framed unknots) due to the choice of normalization. We only need to show invariance under handle sliding.

**Theorem 3.1.** Let  $K$  be a virtual link diagram then  $Z_K(r)$  is invariant under the framed Reidemeister moves, virtual Reidemeister moves, and the virtual Kirby calculus.

In the next few subsections, we introduce some necessary machinery.

In the classical case, the computation of this invariant is simplified by the use of recoupling theory. In the next section, we introduce formulas from recoupling theory [10]. Recoupling theory establishes a relationship between labeled knot diagrams and labeled trivalent graphs with classical and virtual crossings. These formulas allow us to compute the WRT without a full expansion of the Jones polynomial.

### 3.1 Kirby Calculus Invariance

These formulas are obtained from recoupling theory at roots of unity [10]. The formulas simplify the computation of the WRT. They will be used to prove that the WRT is invariant under Kirby calculus.

Consider a virtual link diagram with components  $K_1; K_2 :: K_n$ . We cable component  $K_i$  with  $a_i$  strand and attach a J-W projector. This virtual link diagram can be regarded as a collection of labeled trivalent graphs (each with one edge and no vertices) with classical and virtual crossings. We introduce some formulas obtained from recoupling theory [8]. These formulas describe identities between sums of bracket evaluations of labeled trivalent graphs. A full derivation of each formula can be obtained in [10].

Given a trivalent vertex with labels  $a; b$ , and  $c$  coming into the vertex, we translate this into an expression of J-W projectors. We connect the internal

lines as indicated in figure 17. Note that  $i + j = a$ ,  $j + k = b$ , and  $k + i = c$  where  $i, j$ , and  $k$  are non-negative integers. In order for such a construction to be made:  $a + b + c$  is even,  $a + b \geq c$ ,  $b + c \geq a$ , and  $c + a \geq b$ . These conditions are an admissibility condition for translating any trivalent vertex into projectors for evaluating the colored Jones polynomial for any value of  $a$ . We now give a more technical definition of admissibility for evaluation at roots of unity.

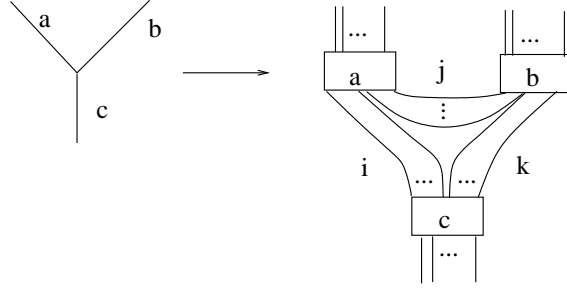


Figure 17: Associating projectors to a trivalent vertex

Fix an integer  $r \geq 2$  and let  $A = e^{\frac{2\pi i}{r}}$ . The quantum factorial is a factorial product based on  $A$ . Let  $0 \leq m \leq r - 1$ . The  $m^{\text{th}}$  quantum factorial is denoted by  $[m]!$ . Now,

$$\begin{aligned} [n] &= (A - 1)^{n-1} A^{-\frac{n-1}{2}} \\ [0]! &= 1 \text{ and } [1]! = A - 1 \\ [m]! &= [m][m-1]! \dots [1]! \end{aligned}$$

For  $r$ , an admissible triple is a set of three non-negative integers such that:

- i)  $a + b + c \geq 2r - 4$  and is even
- ii)  $a + b \geq c$
- iii)  $a + c \geq b$
- iv)  $b + c \geq a$

We recall the  $r$ -net formula,  $(a; b; c)$ . Let  $a; b; c$  be an admissible triple and let  $m = \frac{a+b-c}{2}$ ,  $n = \frac{a+c-b}{2}$ , and  $p = \frac{b+c-a}{2}$  then

$$(a; b; c) = (A - 1)^{m+n+p} \frac{[m+n+p+1]![m]![n]![p]}{[m+n]![n+p]![p+m]} \quad (4)$$

The labeled trivalent diagram shown in figure 18 is referred to as a  $r$ -net. The virtual link diagram represented by the  $r$ -net diagram is pictured on the right (by using the prescription for replacing trivalent vertices with projectors and reducing them). The Jones polynomial of this virtual link diagram is  $(a; b; c)$ .

Note that we can only construct the link diagram corresponding to a  $r$ -net if  $(a; b; c)$  is an admissible triple.

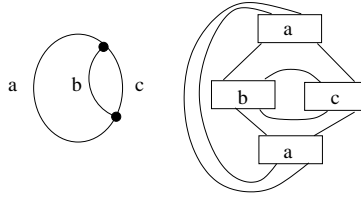


Figure 18: Net Graph

The formula shown in figure 19 (a special case of the recoupling formulas from section 5) expresses the fact that the bracket evaluation of a diagram with two nearby arcs can be replaced with the bracket evaluation of the sum of diagrams obtained by the indicated graphical insertion.

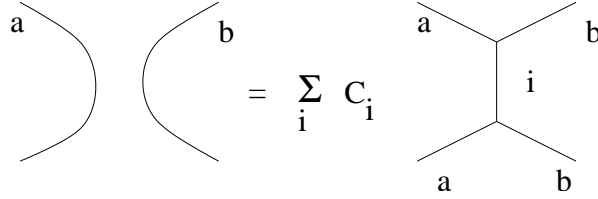


Figure 19: Graph fusion

The coefficients  $C_i$  in this sum are:

$$C_i = \frac{i}{(a;b;i)}; \quad (5)$$

We can only construct the corresponding virtual link diagram when  $(a;b;i)$  is an admissible triple.

These formulas simplify the computation of the WRT of a virtual link diagram.

To prove that the normalized WRT of a virtual knot diagram is unchanged by the virtual Kirby calculus, we need only demonstrate that the WRT is unchanged by handle sliding. We prove the following lemma:

**Lemma 3.2.** Suppose that  $hK^{\dagger}i$  satisfies the conditions shown in figure 20. Then  $hK^{\dagger}i$  is invariant under handle sliding.

**Proof:**

Let  $K_1$  and  $K_2$  be two disjoint components of a virtual knot diagram. Let  $G_1$  denote the cabled  $K_1 \# K_2$  with J-W projectors attached as illustrated in figure 21.

We handle slide  $K_1$  over the knot  $K_2$  to obtain the diagram  $G_4$ . We will show that  $hG_1^{\dagger}i = hG_4^{\dagger}i$ .



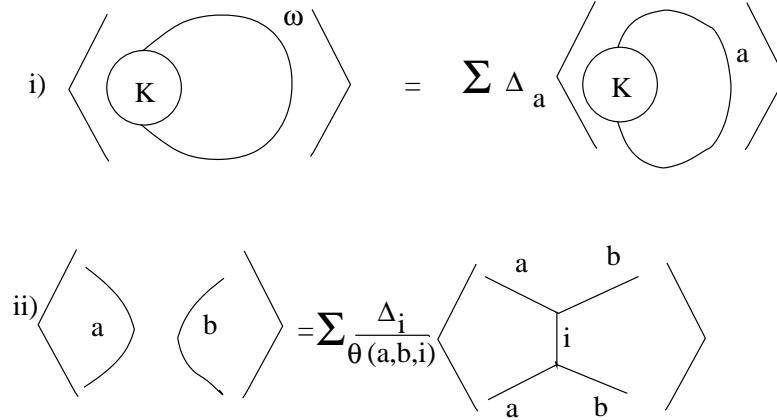


Figure 20: Conditions for Lemma 3.2

Fix  $r \geq 2$  and let  $I = \{0, 1, \dots, r-2\}$ . Then:

$$hG_1^I = \sum_{a,b \in I} \sum_{i \in I} \Delta_i h(K_1 \cup K_2)^{(a,b)}_i$$

Fix  $a$  and consider the sum :

$$\sum_{b \in I} \sum_{i \in I} \Delta_i h(K_1 \cup K_2)^{(a,b)}_i \quad (6)$$

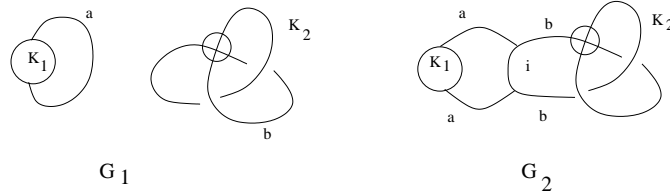


Figure 21: Recoupling move for the handle slide

Perform fusion on  $K_1$  and  $K_2$  and obtain the new diagram  $G_2$ . Now :

$$\sum_{b \in I} \sum_{i \in I} \Delta_i hG_1^{(a,b)}_i = \sum_{b \in I} \sum_{i \in I} \Delta_i \frac{i}{(a,b,i)} hG_2^{(a,b,i)}_i$$

We slide the upper vertex of this graph until we obtain the diagram  $G_3$  as shown in Figure 22. Sliding this edge corresponds to a sequence of Reidemeister II, III and virtual Reidemeister moves.

As a result,

$$\sum_{b \in I} \sum_{i \in I} \Delta_i hG_1^{(a,b)}_i = \sum_{b \in I} \sum_{i \in I} \Delta_i \frac{a \cdot b \cdot i}{(a,b,i)} hG_3^{(a,b,i)}_i \quad (7)$$

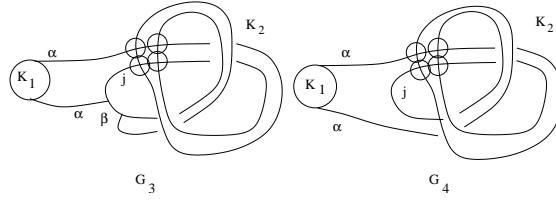


Figure 22: Recoupling diagrams after fusion

Applying the inverse of the fusion formula to the previous equation:

$$\sum_{b \in I} X_{a \ b} h_{G_1}^{(a \ b)} i = \sum_{i \in I} X_{a \ i} h_{G_4}^{(a \ i)} i$$

Now :

$$\sum_{a \ b \in I} X_{a \ b} h_{G_1}^{(a \ b)} i = \sum_{a \ i \in I} X_{a \ i} h_{G_4}^{(a \ i)} i \quad (8)$$

Hence,  $h_{G_1}^{(i \ i)} i = h_{G_4}^{(i \ i)} i$  ■

## 4 Examples

In this section, we compute the WRT of the two virtual knot diagrams,  $K$  and  $\hat{K}$ , shown in figure 23.

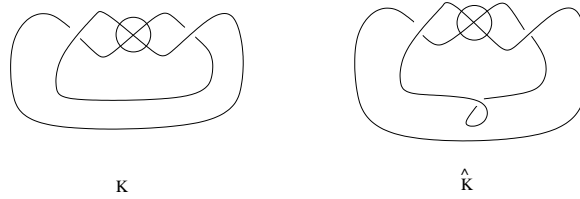


Figure 23: Virtual knot diagrams,  $K$  and  $\hat{K}$

Both  $K$  and  $\hat{K}$  have fundamental group  $\mathbb{Z}$ . The three-manifold groups of these diagrams are

$$M(K) = \mathbb{Z}_2 \text{ and } M(\hat{K}) = 1:$$

Note that  $M(S^1 \times S^2) = \mathbb{Z}$  and  $M(S^3) = 1$ .

To compute the WRT of these virtual knot diagrams, we recall the following formulas from recoupling theory. These formulas establish a correspondence between labeled trivalent graphs and sums of virtual knot diagrams with coefficients in  $\mathbb{C}$ .

We define the tetrahedral net formula. Let  $a; b; c; d; e$  and  $f$  be non-negative integers.

$$\text{Tet} \begin{matrix} a & b & e \\ c & d & f \end{matrix} = \frac{G}{E} \prod_{i,j}^Y \frac{(1)^s [s+1]!}{[s+a_i]! [b_j-s]!} \quad (9)$$

such that

$$\begin{aligned} E &= [a]![b]![c]![d]![e]![f]! & G &= \prod_{i,j}^Y [b_j - a_i]! \\ a_1 &= \frac{(a+d+e)}{2} & a_2 &= \frac{(b+c+e)}{2} \\ a_3 &= \frac{(a+d+f)}{2} & a_4 &= \frac{(b+c+f)}{2} \\ b_1 &= \frac{(a+c+e+f)}{2} & b_2 &= \frac{(b+d+e+f)}{2} \\ b_3 &= \frac{(a+b+c+d)}{2} \\ m &= \min\{a_1; a_2; a_3; a_4\} & M &= \max\{b_1; b_2; b_3\} \end{aligned}$$

The trivalent graph shown on the left in figure 24 corresponds to the link diagram shown on the right. The Jones polynomial of this virtual link diagram is

$$\text{Tet} \begin{matrix} a & b & e \\ c & d & f \end{matrix} : \quad (10)$$

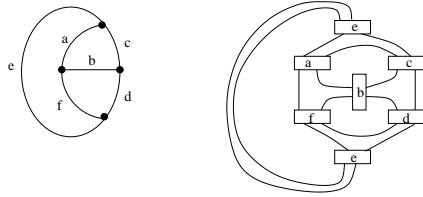


Figure 24: Tetrahedral net graph

We may remove a classical crossing from a trivalent graph using the following formula. We define the weight coefficient:

$$\frac{ab}{c} = (-1)^{\frac{a+b-c}{2}} A^{\frac{a(a+2)+b(b+2)-c(c+2)}{2}} :$$

The complex conjugate of  $\frac{ab}{c}$  is :

$$\frac{ab}{c} = (-1)^{\frac{a+b-c}{2}} A^{\frac{a(a+2)+b(b+2)-c(c+2)}{2}} : \quad (11)$$

We remove a simple twist from the diagram as shown in figure 25. The equalities indicate that the bracket evaluations of the two diagrams are equivalent.

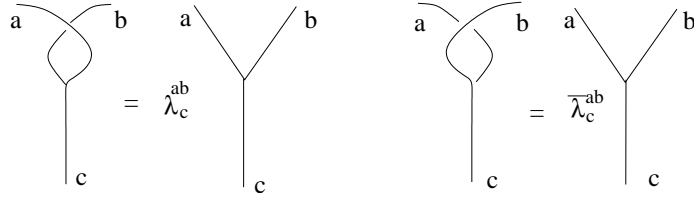


Figure 25: Graphical  $\lambda_c^{ab}$

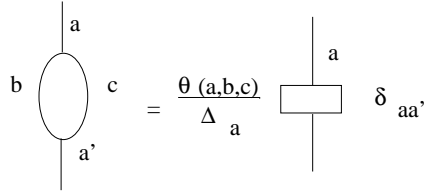


Figure 26: Bead removal formula

We may also simplify a trivalent graph using the formula shown in figure 26. We refer to this simplification as a bead removal.

The following formula equates a classical crossing with a weighted sum of trivalent subgraphs. We exchange a crossing for a sum of trivalent subgraphs as shown in figure 27,

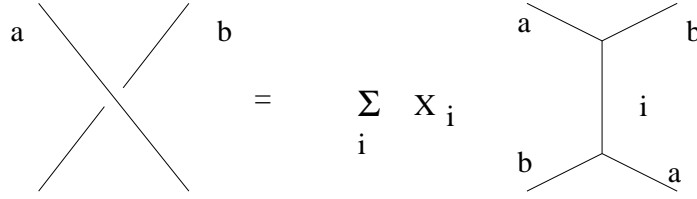


Figure 27: Crossing expansion formula

where

$$X_i = \frac{i_i^{ab}}{(a;b;i)} :$$

#### 4.1 Computations

Let  $K$  and  $\hat{K}$  be the diagrams shown in figure 23. We compute  $hK^! i$  and  $h\hat{K}^! i$ . Applying the definition of the WRT,

$$hK^! i = \sum_{i,j;a} \frac{X}{a} hK^a i$$

$$h\hat{K}^! i = \sum_{i,j;a} \frac{X^a}{a} h\hat{K}^a i$$

Now, we use the formulas obtained from recoupling theory to transform the virtual knot diagrams  $K$  and  $\hat{K}$  into the trivalent graph  $G$  shown in figure 28. As a result:

$$hK^! i = \sum_{i,j;a} \frac{X}{a} \frac{i \ j}{(a;a;i) (a;a;j)} \begin{smallmatrix} aa & aa \\ i & j \end{smallmatrix} hG i$$

$$h\hat{K}^! i = \sum_{i,j;a} \frac{X}{a} \frac{i \ j}{(a;a;i) (a;a;j)} \begin{smallmatrix} aa & aa \\ i & j \end{smallmatrix} \begin{smallmatrix} aa \\ 0 \end{smallmatrix} hG i:$$

Note that  $(a;i;j)$  is not an admissible triple unless  $i = j$ . Then:

$$hK^! i = \sum_{i;a} \frac{X}{a} \frac{i \ i}{(a;a;i)^2} hG i$$

$$h\hat{K}^! i = \sum_{i;a} \frac{X}{a} \frac{i \ i}{(a;a;i)^2} \begin{smallmatrix} aa \\ i \end{smallmatrix} \begin{smallmatrix} aa \\ 0 \end{smallmatrix} hG i$$

Applying the net identity, we obtain the graph,  $G^0$ , shown in figure 29.

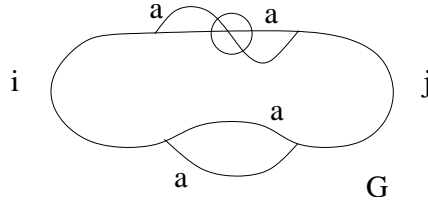


Figure 28: Graph obtained from  $K$  and  $\hat{K}$

Now,

$$hK^! i = \sum_{i;a} \frac{X}{a} \frac{i}{(a;a;i)} \begin{smallmatrix} aa \\ i \end{smallmatrix} \begin{smallmatrix} aa \\ 0 \end{smallmatrix} hG^0 i$$

$$h\hat{K}^! i = \sum_{i;a} \frac{X}{a} \frac{i}{(a;a;i)} \begin{smallmatrix} aa \\ i \end{smallmatrix} \begin{smallmatrix} aa \\ 0 \end{smallmatrix} hG^0 i$$

We determine for which values the triple,  $(a;a;i)$ , is admissible. We then compute the Jones polynomial of the virtual link diagrams corresponding to the labeled graph,  $G^0$ .

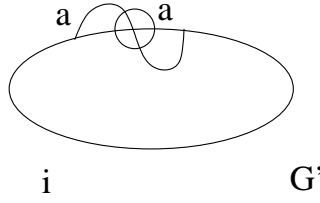


Figure 29: Reduced graph obtained from  $G$

	$a = 0$	$a = 1$
$i = 0$	1	$A^2 \ A^{-2}$
$i = 1$	0	0

Table 1: Jones polynomial of the graph  $G^0$ ,  $r = 3$

We indicate these values in table 4.1. If the triple  $(a; a; i)$  is not admissible, we have entered a zero in the corresponding table entry.

For  $r = 3$ :

$$hK^1 i = \frac{\frac{2}{0} \binom{00}{0}^2 hG^0 i}{(0; 0; 0)} + \frac{\frac{2}{0} \binom{11}{0}^2 hG^0 i}{(1; 1; 0)}$$

and

$$h\hat{K}^1 i = \frac{\frac{2}{0} \binom{00}{0}^3 hG^0 i}{(0; 0; 0)} + \frac{\frac{2}{0} \binom{11}{0}^3 hG^0 i}{(1; 1; 0)}.$$

Now,

$$hK^1 i = 0$$

$$h\hat{K}^1 i = 1 + i$$

We set  $r = 4$ . We determine for what values  $(a; a; i)$  is an admissible triple. We then compute the Jones polynomial of the virtual link diagram corresponding to the graph  $G_2$ .

We compute  $hK^1 i$  when  $r = 4$ .

$$hK^1 i = \frac{\frac{2}{0} \binom{00}{0}^2 hG^0 i}{(0; 0; 0)} + \frac{\frac{2}{0} \binom{11}{0}^2 hG^0 i}{(1; 1; 0)} + \frac{\frac{2}{0} \binom{22}{0}^2 hG^0 i}{(2; 2; 0)} + \frac{\frac{2}{2} \binom{11}{2}^2 hG^0 i}{(1; 1; 2)}$$

	$a = 0$	$a = 1$	$a = 2$
$i = 0$	1	$A^2 \ A^{-2}$	$(A^2 \ A^{-2})^2$
$i = 1$	0	0	0
$i = 2$	0	$A^2 \ A^{-2}$	0

Table 2: Jones polynomial of the graph  $G^0$ ,  $r = 4$

Similarly, we compute the WRT of  $\hat{K}$  when  $r = 4$ .

$$\begin{aligned} h\hat{K}^1 i = & \frac{\frac{2}{0} \begin{pmatrix} 00 \\ 0 \end{pmatrix}^3 hG^0 i}{(0;0;0)} + \frac{\frac{2}{0} \begin{pmatrix} 11 \\ 0 \end{pmatrix}^3 hG^0 i}{(1;1;0)} \\ & + \frac{\frac{2}{0} \begin{pmatrix} 22 \\ 0 \end{pmatrix}^3 hG^0 i}{(2;2;0)} + \frac{\frac{2}{2} \begin{pmatrix} 11 \\ 2 \end{pmatrix}^2 \frac{11}{0} hG^0 i}{(1;1;2)} \end{aligned}$$

We determine that

$$hK i = 1.29289 + 1.70711i$$

$$h\hat{K} i = 1.23044 + 0.92388i$$

The virtual knot diagram  $K$  has  $b_+(K) = 0$  and  $b_-(K) = 0$  implying  $n(K) = 1$ . Now, we normalize the WRT and determine that:

$$Z_K(3) = 0$$

$$Z_{\hat{K}}(3) = 0.707107i$$

We determine that the normalized WRT when  $r = 4$ .

$$Z_K(4) = 0.517982 + 0.135299i$$

$$Z_{\hat{K}}(4) = 0.331106 + 0.195807i$$

## 5 Recoupling Theory and Virtual Knot Diagrams

Recall the recoupling theorem [10].

**Theorem 5.1 (Recoupling Theorem).** A single labeled trivalent graph is equivalent to a sum of labeled trivalent graphs with coefficients in  $\mathbb{C}$  as illustrated in figure 30. Note that

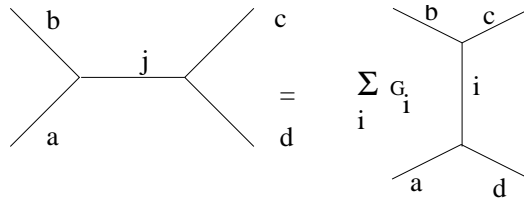


Figure 30: Graph exchange (exchanging a H-shaped graph for an I-shaped graph)

$$G_i = \frac{\text{Tet} \begin{array}{ccc} a & b & i \\ c & d & j \end{array}}{(a;d;i) (b;c;j)} \quad (12)$$

**Proof:** [10]. ■

Remark 5.1. One of the formulas given in section 3 is a special case of the recoupling theorem. In particular, if  $j = 0$ , we obtain the fusion formula from section 3.

We now prove a theorem that demonstrates a sum of H-shaped trivalent graphs can be rewritten as a sum of I-shaped trivalent subgraphs. This procedure gives the appearance of sliding edges past the vertices of the trivalent graph. Using the recoupling theorem, we may transform any trivalent graph without virtual crossings into a sum of weighted string of beads graphs as illustrated in figure 31.

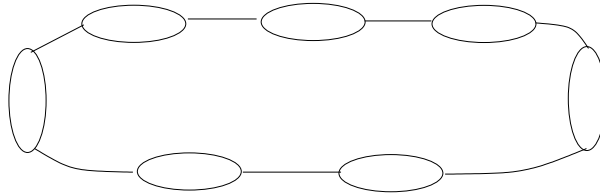


Figure 31: Example: String of Beads Graph

Lemma 5.2 (Trivalent Graphs). A classical knot diagram may be transformed into a string of beads graph by replacing each classical crossing with a trivalent subgraph and applying the recoupling theorem.

Remark 5.2. This result follows from the fact that thickening an I-shaped and a H-shaped graph produces two homeomorphic surfaces. The surface produced by thickening any planar graph is a  $n$ -punctured sphere. The punctured sphere deformation retracts to a string of beads graph after homeomorphism. We will generalize this approach to show that virtual link diagrams correspond to a specific type of trivalent graphs. This lemma will be proved as a sub case of Lemma 5.3. Refer to [10], p. 115.

The recoupling formula allows us to translate any planar trivalent graph (no virtual crossings) into a string of beads graph. This fact restricts the types of subgraphs that occur (in graphs obtained from classical link diagrams) to a small number of possibilities. As a result, we need only compute formulas that determine the WRT of the classical tangle diagrams that correspond to these labeled subgraphs. In particular, it is sufficient to compute the coefficients that correspond to the insertion and deletion of  $\bar{\mu}$ -net subgraphs.

The reduction to a simple string of beads does not hold for virtual link diagrams. We can remove all classical crossings from the diagram by exchanging the classical crossings for H or I shaped trivalent subgraphs, and obtain a trivalent graph with only virtual crossings. However, we can not remove all virtual crossings by applying the recoupling theorem. For example, the graph shown in figure 32 can not be reduced to a trivalent graph without virtual crossings.



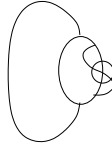


Figure 32: Unreduceable super bead

The reduced form of a virtual knot diagram is similar to a string of beads graph but includes three different types of beads. The reduced form of the virtual knot diagram is a string of super beads, twisted beads and beads. We illustrate the possible three bead types from the virtual case in Figure 33.

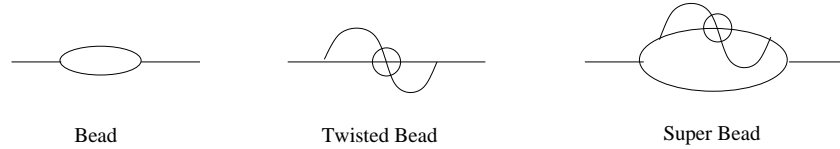


Figure 33: Beads types formed by virtual knot diagrams

We prove that the WRT of a virtual link diagram is equal to a weighted sum of the Jones polynomial of virtual link diagrams. The virtual link diagrams are indicated by labeled virtual string of beads graphs. These string of bead graphs are obtained from the virtual link diagram by applying the recoupling theorem and crossing exchange. We first prove a lemma that demonstrates any trivalent graph with virtual crossings can be transformed into a string of the three bead types by sliding edges.

**Lemma 5.3 (Graphical Lemma).** Any trivalent graph with virtual crossings may be reduced to a trivalent string of beads graph with three possible types of beads: the standard bead, twisted bead, and super bead. This graph will contain at most one twisted bead.

**Proof:** Thicken the graph so that the graph is the core of a compact oriented surface,  $T(G)$ . An example of a graph and its corresponding thickened surface is shown in Figure 34. Note that we may apply homeomorphisms to these surfaces and the surfaces do not depend on the choice of embedding in 3 dimensional space. The two surfaces on the right hand side of Figure 34 are equivalent.

Note that if the graph,  $G$  has  $2n$  vertices, then  $G$  has  $3n$  edges since the graph is trivalent. The Euler characteristic of the surface,  $T(G)$  is  $-n$  (since  $G$  is a deformation retract of  $T(G)$ ). Without loss of generality, we assume that the surface has  $k$  boundary components.

Recall the following theorem from [5].

**Theorem 5.4 (Surface Classification).** Let  $M$  be a connected, compact, orientable surface of Euler characteristic  $\chi$ . Suppose  $\partial M$  has  $k \geq 0$  boundary components. Then  $\chi + k$  is even. Let  $p = 1 - \frac{(\chi + k)}{2}$  then  $M$  is diffeomorphic to

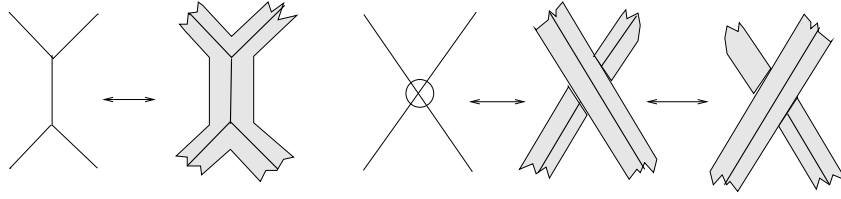


Figure 34: Thickened graph

the surface obtained from an orientable surface of genus  $p$  by the removal of the interiors of  $k$  disjoint disks.

Applying Theorem 5.4,  $(S) + k = n + k$  and  $n + k$  is even. Let  $p = 1 - \frac{n+k}{2}$ . We observe that  $T(G)$  is the connected sum of  $p$  tori with  $k$  punctures. Each torus component contributes a handle pair. Each handle pair corresponds to either a twisted bead or part of a super bead depending on the number of punctures. Each punctured disk forms either a plain bead or part of a super bead as shown in figures 35 and 36.

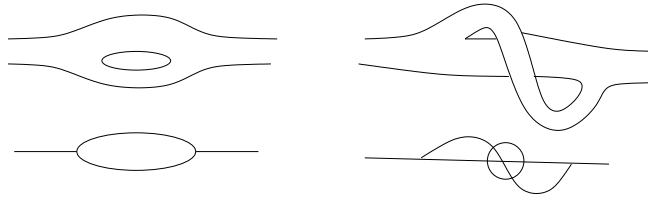


Figure 35: Surfaces corresponding to the standard bead and the twisted bead

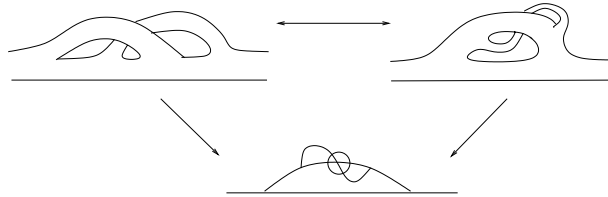


Figure 36: Surfaces corresponding to the super bead

For example, a surface with one handle pair and one puncture corresponds to a single twisted bead on a loop (the graph shown in figure 32). The connected sum of three tori with one puncture and its corresponding graph are shown in figure 37.

After isotopy, any surface that is the connected sum of  $p$  tori with  $k$  punctures may be regarded as a series of  $p$  handle pairs attached to a disk with  $k - 1$  punctures. As a result, these surfaces deformation retract to a string of beads

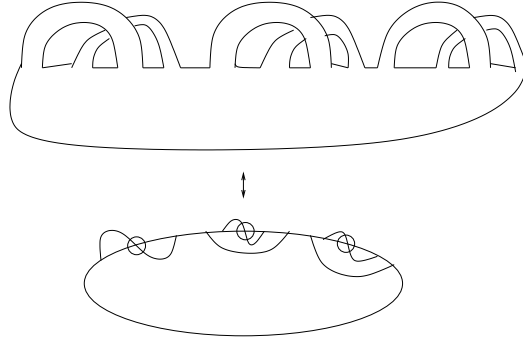


Figure 37: A surface and its corresponding graph

type trivalent graph with standard beads, twisted beads, and a single super bead. ■

**Theorem 5.5 (Virtual Recoupling Theorem).** Let  $K$  be a labeled virtual link diagram. Using the recoupling theorem and crossing expansion, we may transform the virtual link diagram into a sum of labeled trivalent, string of beads graphs with coefficients in  $\mathbb{C}$ . The WRT of the labeled virtual link diagram is equal to the WRT of the sum of weighted trivalent graphs.

**Proof:** From the previous theorem, it is clear that we can transform a virtual link diagram into a string of beads graph using the recoupling theorem and crossing expansion without coefficients. After determining this sequence of transformations, apply the appropriate coefficients and labels indicated by the recoupling theorem, the crossing expansion formula, and the initial labeling of the link. ■

## 5.1 Obstruction to Weight Formulas

Recall that the  $n^{\text{th}}$  Jones-Wenzl idempotent has the property that  $T_n U_i = 0$  for any elementary  $n$ -tangle  $U_i$ . We cannot easily extend the evaluation formulas given earlier in this paper because the Jones-Wenzl projector does not necessarily have the property that  $T_n P_n = 0$  when  $P_n$  is a  $n$ -tangle with only virtual crossings. In the classical case, we relied on this fact to simplify the recursive formulas. The recursion formulas needed to determine the value of the Jones polynomial of  $T_n P_n$  depend on the position of the virtual crossings. The evaluation of these formulas requires that we know the Jones polynomial of the closure of  $T_{n-1} P_{n-1}$  for all  $(n-1)$ -tangles  $P_{n-1}$  containing only virtual crossings. We prove two theorems that indicate the complexity involved in computing the Jones polynomial of  $T_n P_n$ .

**Theorem 5.6.** The  $n^{\text{th}}$  J-W projector,  $T_n$ , does not annihilate all  $n$ -tangles  $P_n$  with only virtual crossings.

To prove Theorem 5.6 we need only demonstrate that  $T(T_n E) \neq 0$  where  $E$  is a  $n$ -tangle with a single virtual crossing. We postpone this proof until after the proof of Lemma 5.9.

We introduce the following propositions preliminary to the proof of Theorem 5.6. The formulas in these propositions determine the number of the Jones polynomial of the closure  $T_n P_n$ .

Proposition 5.7. If  $P$  is a  $(n-1)$ -tangle with only virtual crossings, we construct a  $n$ -tangle,  $P_n$ , by attaching an additional strand on the right. Then the Jones polynomial of the closure of  $T_n P$  is determined by the following formula.

$$T_n P = T_{n-1} P - \frac{n-2}{n-1} T_{n-1} P$$

Proof: Apply the recursion relation shown in Figure 38. ■

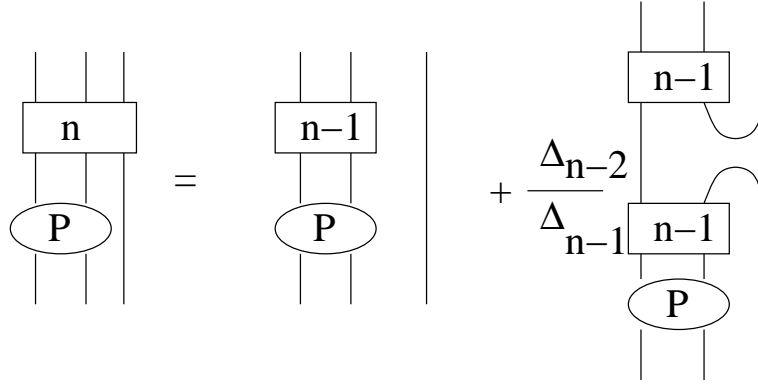


Figure 38: Diagrammatic proof of Proposition 5.7

Proposition 5.8. Let  $P$  be a  $n$ -tangle with only virtual crossings. We compute  $T_n P$  recursively, and the depth of the recursion equation depends on the initial position of the rightmost strand in the  $n$ -tangle  $P$ .

Proof: Let  $P$  be an  $n$ -tangle with only virtual crossings. We compute  $T_n P$  recursively as shown in Figures 38 and 39. We expand the diagram as indicated in Figure 39. The complexity of the recursion depends on the virtual crossings in  $P$ . ■

Remark 5.3. The question of handling this recursion in a systematic way is an interesting research question.

Lemma 5.9. Let  $E$  denote the  $n$ -tangle with a single virtual crossing involving only the 1<sup>st</sup> and the 2<sup>nd</sup> strands. Then:

$$\text{dhcl}(T_n E) = (d + \frac{n-2}{n-1}) :: (d + \frac{1}{2})(d-1)$$

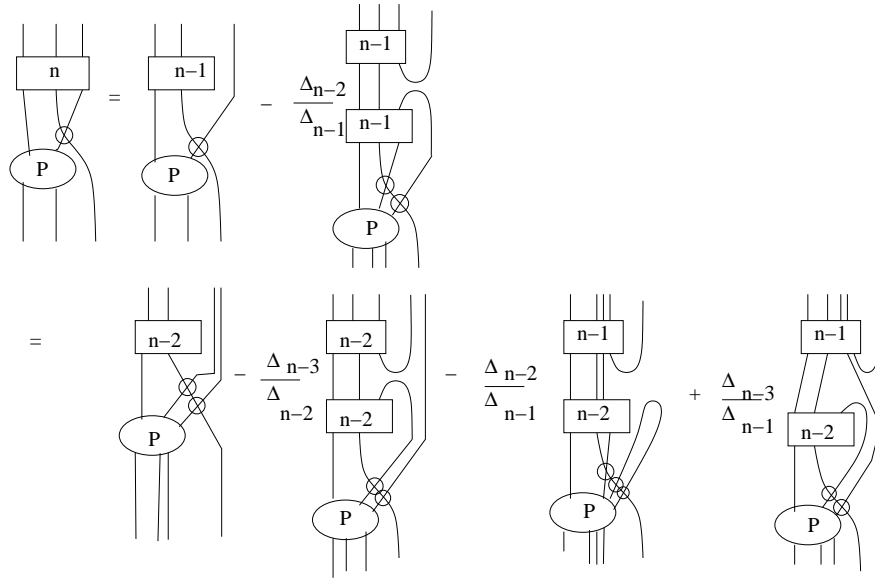


Figure 39: Diagrammatic proof of Proposition 5.8

Proof: We apply formula from Proposition 5.7 to  $T_n E$ . We calculate  $\text{hcl}(T_n E) = 1 - d$ . ■

We now prove Theorem 5.6.

Proof of Theorem 5.6: If  $T_n$  is an idempotent, then  $T_n E = 0$ . However,  $\text{hcl}(T_n E) \neq 0$  indicating that  $T_n E$  is not the empty diagram. ■

The algebra generated by extending  $n$ -tangle diagrams by including virtual crossings is a diagrammatic version of the Brauer algebra. Note that each classical  $n$ -tangle diagram is expanded (via the bracket) into an element of the Temperley-Lieb algebra. It is this extension of the Temperley-Lieb algebra by virtual elements that is isomorphic to the Brauer algebra. The Brauer algebra is described in [1]. We would like to understand the structure of the Jones-Wenzl projectors in the context of the Brauer algebra. Results in this area would help in understanding the extension of the WRT invariant that we have discussed in this paper.

Acknowledgement. This effort was sponsored in part by the Office of the Dean at the United States Military Academy. The U.S. Government is authorized to reproduce and distribute reprints for Government purposes notwithstanding any copyright annotations thereon. The views and conclusions contained herein are those of the authors and should not be interpreted as necessarily representing the official policies or endorsements, either expressed or implied, of the United States Military Academy or the U.S. Government. (Copyright 2004.) Much of this effort was sponsored by the Defense Advanced Research Projects Agency (DARPA) and Air Force Research Laboratory, Air Force Materiel Command, USAF, under agreement F30602-01-2-05022. The U.S. Government

ment is authorized to reproduce and distribute reprints for Government purposes notwithstanding any copyright annotations thereon. The views and conclusions contained herein are those of the authors and should not be either expressed or implied, of the Defense Advanced Research Projects Agency, the Air Force Research Laboratory, or the U.S. Government. (Copyright 2004.) It gives the second author great pleasure to acknowledge support from NSF Grant DMS-0245588, and to thank the Stanford Linear Accelerator Theory Group, the University of Waterloo and the Perimeter Institute for hospitality during the preparation of this research.

## References

- [1] Georgia Benkart, Commuting actions | a tale of two groups, *Contemporary Mathematics*, American Mathematical Society, Vol. 194, p. 1-46, 1996, Lie algebras and their representations (Seoul, 1995)
- [2] J. Scott Carter, Seiichi Kamada, and Masahico Saito, Stable equivalence of knots on surfaces and virtual knot cobordisms, *Knots 2000 Korea*, Vol. 1 (Yongpyong), *J. Knot Theory Ramifications* 11 (2002), no. 3, 311-32
- [3] Heather A. Dye and Louis H. Kauffman, Minimal surface representations of virtual knots and links, [www.arxiv.org](http://www.arxiv.org), GT/0401035
- [4] Mikhail Gussarov, Michael Polyak, and Oleg Viro Finite Type Invariants of Classical and Virtual Knots, *Topology* 39 (2000), no. 5 p. 1045-1068
- [5] Morris W. Hirsch, *Differential Topology*, Springer-Verlag, Graduate Texts in Mathematics, 1977
- [6] Naoko Kamada and Seiichi Kamada, Abstract link diagrams and virtual Knots, *Journal of Knot Theory and its Ramifications*, Vol. 9 No. 1, p. 93-109, World Sci. Publishing, 2000
- [7] Louis H. Kauffman, Detecting Virtual Knots, *Atti del Seminario Matematico e Fisico dell'Universita di Modena*, Vol. 49, suppl., p. 241-282, Univ. Modena, 2001
- [8] Louis H. Kauffman, *Knots and Physics*, Series on Knots and Everything, Vol. 1, World Scientific, 1991, 1994, 2001
- [9] Louis H. Kauffman, Virtual Knot Theory, *European Journal of Combinatorics*, Vol. 20, No. 7, p. 663-690, Academic Press, 1999
- [10] Louis H. Kauffman and Sostenes L. Lins, Temperley-Lieb Recoupling Theory and Invariants of 3-Manifolds, *Annals of Mathematics Studies*, Princeton University Press, 1994
- [11] Greg Kuperberg, What is a Virtual Link?, *Algebr. Geom. Topol.* 3 (2003), p. 587-591 (electronic) [www.arxiv.org](http://www.arxiv.org), GT/0208039

- [12] Vassily O .M anturov, Kau m an-Like Polynom ialand Curves in 2-Surfaces  
Journal of Knot Theory and its Ram i cations, Vol. 12 (2003), no. 8, p.  
1145-1153
- [13] V iktor V .P rasolov and A lexei B . Sossinsky, Knots, Links, Braids and  
3-M anifolds; A n Introduction to New Invariants in Low -D im ensional Topol-  
ogy, A m erican M athem atical Society, Translations of M athem atical M ono-  
graphs, 1996
- [14] N ikolai Yu Reshetikhin and V ladin ir G .Turaev, Invariants of 3-m anifolds  
via link polynom ials and quantum groups, Inventiones M athem aticae, Vol.  
103, No. 3, p. 547-597 , Springer, 1991
- [15] N ikolai Yu Reshetikhin and V ladin ir G .Turaev, Ribbon Graphs and their  
invariants derived from quantum groups, Com m unications in M athem ati-  
cal Physics, Vol. 127, No. 1, p. 1-26, Springer, 1990,
- [16] Edward W itten, Quantum eld theory and the Jones polynom ial, Braid  
group, knot theory and statistical m echanics, II, p. 361-451, Adv. Ser.  
M ath. Phys., 17, W orld Sci. Publishing 1994